# AC loss calculation on a 6.5 MVA/25 kV HTS traction transformer with hybrid winding structure

W. Song, Z. Jiang, *Senior member, IEEE*, M. Staines, S. Wimbush, R. Badcock, *Senior member, IEEE*, and J. Fang

***Abstract* —HTS wire cost is a critical factor for successful commercialization of HTS traction transformer technology. Wire cost might be minimized without significantly increasing AC loss by introducing a hybrid winding structure: the end-part of the windings is wound with high-cost high-$I_c$ wires; the central-part of the windings is wound with low-cost low-$I_c$ wires. We report AC loss simulation results on HTS windings with both HV and LV windings wound with REBCO wires. The 2D axisymmetric FEM simulation was carried out using *H*-formulation. The HV windings are wound with 4 mm-wide wires and LV windings are wound with 8/5 (eight 5 mm – wide strands) Roebel cables. Both HV and LV windings have a hybrid structure in order to reduce the wire cost. Flux diverters are placed at the end of the windings to reduce AC loss. Significant HTS wire cost reduction could be achieved without compromising AC loss by using hybrid windings. This may help commercialize HTS traction transformer technology.**

***Index Terms*—AC loss, traction transformer, hybrid winding structure, wire cost.**

## I. Introduction

TRACTION transformers are key components for the Chinese high speed train system [1] - [4]. Since 2018 Beijing Jiaotong University has been leading a six-party project to develop a single-phase 6.5 MVA HTS traction transformer [5] - [7]. The ultimate goal of the project is to replace the conventional traction transformers, which are heavy, have low efficiency, and are oil-cooled - a significant fire risk. The HTS transformer is expected to demonstrate superior performance over conventional transformers with oil-immersed copper-windings, achieving 99% efficiency and 3 tonne total system weight compared to 95% efficiency and approximately 6 tonne weight for conventional transformers. Minimization of AC loss in the HTS windings is critical to achieve both these efficiency and system weight targets [6], demanding high $I_c$ HTS wire. On the other hand, wire cost is one of the major obstacles preventing commercialization of HTS power equipment. It is therefore a huge challenge to realize a high-performance, economic transformer, reducing wire cost whilst keeping the AC loss low.

TABLE I
SPECIFICATIONS OF WINDING DESIGN

| Parameter | Value |
|---|---|
| Winding length $L$ (m) | 1 |
| Number of turns in each HV winding disc | 14 |
| Number of discs stacked to make the HV winding per unit | 116 |
| Number of layers of 8-strand Roebel cable in LV winding | 3 |
| Number of turns in one layer in LV winding | 40 |
| Number of total turns per unit in HV winding | 1624 |
| Number of total turns per unit in LV winding | 120 |
| Inner diameter of HV winding (mm) | 437 |
| Inner diameter of LV winding (mm) | 285 |
| Axial gap between the two units on each leg of the core (mm) | 20 |
| Short-circuit impedance (%) | 43 |

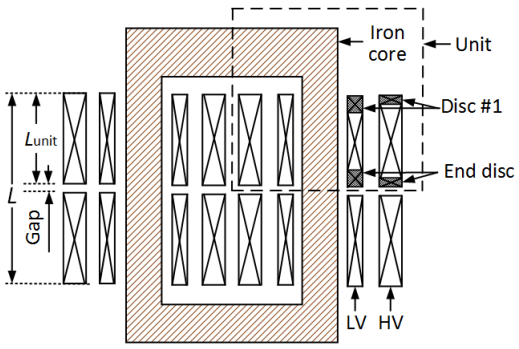


Fig. 1. Schematic of 6.5 MVA traction transformer. The transformer has four units and each consists of HV and LV windings.

The transformer consists of four single-phase 25 kV/1.9 kV HTS windings, operating at 65 K and 50 Hz, each of which drive a motor. A base layout was designed where the transformer has four winding units and each leg of the core has two winding units around it as depicted in Fig. 1 [6]. Each unit comprises one HV winding and one LV winding, respectively. The rated currents for each of the HV and LV windings are 64.25 A and 846 A, respectively. All the winding assemblies will be housed in two individual vacuum-insulated horizontal cryostats and will be cooled by sub-cooled liquid nitrogen in an open-loop cryo-cooling system [6], [8]. Table I lists the specifications of the HV and LV windings.

Manuscript received on September 24, 2019. This work was supported by Ministry of Science and Technology on National Key Research and Development Program of China under Grant No. 2016YFE0201200. *(Corresponding author: Zhenan Jiang.)*

Wenjuan Song is with Department of Electronics and Electrical Engineering, University of Bath, United Kingdom, Robinson Research Institute, Victoria University of Wellington, New Zealand, as well as with School of Electrical Engineering, Beijing Jiaotong University, Beijing, China, 100044 (email: ws603@bath.ac.uk)

Zhenan Jiang, Michael Staines, Stuart C. Wimbush, Rodney A. Badcock are with Robinson Research Institute, Victoria University of Wellington, PO Box 33436, Lower Hutt 5046, New Zealand. (email: zhenan.jiang@vuw.ac.nz)

Jin Fang is with School of Electrical Engineering, Beijing Jiaotong University, Beijing, China, 100044.

In order to deal with high current and minimize AC loss in the LV windings, we use 8/5 Roebel cable (eight 5-mm-wide strands) [9] - [12]. The HV input current to the transformer is 257 Arms, with the windings for each unit, symmetrically connected in parallel, carrying only 64.25 Arms. Therefore, a single 4 mm-wide REBCO superconductor wire can handle the HV current. As in previous transformer AC loss modelling [12, 13], we do not consider the iron core in the simulation.

Both the entire HV and LV windings can be wound with high $I_c$, high quality Fujikura wires, with critical current of 1140 A/cm at 65 K. However, a hybrid coil winding structure can be introduced in the traction transformer to reduce HTS wire cost, i.e. use high $I_c$, higher cost wires in the end part of the HV and LV windings, and low $I_c$, lower cost wires in the majority of the rest of the coil windings. The concept of hybrid winding structure is based on the fact that HTS conductors in different part of a winding experience different magnetic fields: conductors in the end part of the winding are exposed to large radial magnetic field; conductors in the central part of the winding are mainly exposed to parallel magnetic field [14, 15]. As a result, AC loss in the end part of the winding dominates the AC loss of the whole winding, and AC loss in the central part of the winding is negligible [12, 13].

In this paper, we considered hybrid winding structures for HTS traction transformers where the end part of the winding is wound with Fujikura wires with a self-field $I_c$ of 1140 A/cm at 65 K and the central part of the winding is wound with Shanghai Superconductor (SHS) wires with a self-field $I_c$ of 1067 A/cm at 65 K. We designed five configurations for transformer windings including three hybrid windings. The schematics of the windings are shown in Fig. 2. In Conf. #1, HV and LV windings are wound with Fujikura wire only. In Conf. #2, HV and LV windings are wound with SHS wire only. In Confs. #3, #4, and #5, two, four, and six discs of the end parts of both the HV and LV windings are wound with Fujikura wire while the rest of the windings are wound with SHS wire. It is worth noting that the "disc" in the LV winding is Roebel cable. Conf. #6 is the same as Conf. #3 except for the flux diverters arranged near the end of the windings. AC loss in the transformer windings were calculated and compared with each other.

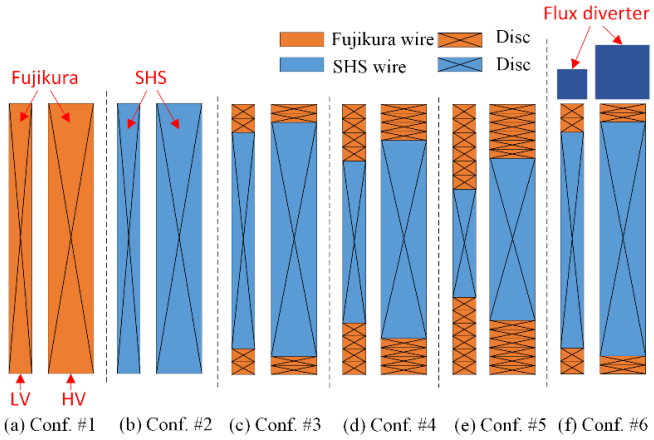


Fig. 2. Schematics of hybrid transformer windings (a) Conf. #1 (b) Conf. #2 (c) Conf. #3 (d) Conf. #4 (e) Conf. #5 and (6) Conf. #6

## II. Numerical Calculation

Calculations have been carried out in a 2D axisymmetric modelling using *H* formulation [13], [16]- [19]. Considering the symmetry of the transformer structure, only one unit of transformer windings was simulated [5, 6]. Fig. 3 shows the schematic of a quarter 2D axisymmetric model for the 6.5 MVA transformer windings.

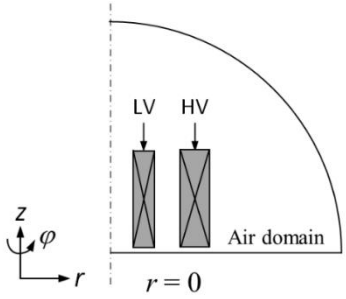


Fig. 3. Schematic of a 2D axisymmetric model for 6.5 MVA transformer (only a quarter model was simulated)

The variables in the model were defined as $\boldsymbol{H} = [H_r, H_z]^T$, where $H_r$ is the radial magnetic field and $H_z$ is the axial magnetic field. We assume that the current only flows in $\varphi$ direction. The function between local electric field $E_\varphi$ and local current density $J_\varphi$ is expressed by Ohm's law,

$$E_\varphi = \rho J_\varphi \tag{1}$$

where $\rho$ is the resistivity of the material. In air region, $\rho_{\text{air}} = 1\ \Omega\text{m}$ was used in the modelling, and in superconducting region, $\rho_{\text{HTS}}$ is derived from *E-J* power law as shown as (2) to indicate the resistivity for superconducting tape.

$$\rho_{HTS} = \frac{E_c}{J_c(B)}\left(\frac{J_\varphi}{J_c(B)}\right)^{(n-1)} \tag{2}$$

Here, power index $n = 25$, $E_c = 10^{-4}$ V/m was used in the work. $J_c(B)$ is the critical current density dependence on external magnetic field and it normally can be obtained from the measured $I_c(B)$ data divided by the cross-section area of the superconductor, *S*. A modified Kim model [20] for the $J_c(B)$ performance was implemented in the modelling, as shown in equation (3),

$$J_c(B) = \frac{I_{c0}}{S}\left(1 + \frac{k^2 {B_{\text{para}}}^2 + {B_{\text{perp}}}^2}{{B_0}^2}\right)^{-\alpha} \tag{3}$$

where $I_{c0}$ is the self-field critical current at a certain temperature; $B_0$, $k$ and $\alpha$ were the fitting parameters obtained by comparing the fitted $I_c(B)$ curves and measured ones under different applied magnetic fields. In this work, $B_{\text{perp}}$ is the radial magnetic field $B_r$, and $B_{\text{para}}$ is the axial magnetic field $B_z$.

Figs. 4(a) and 4(b) show the measured and fitted critical current of both Fujikura and SHS wires under perpendicular magnetic field and parallel magnetic fields using (3). The fitted $I_c(B)$ curves show good agreement with the measured ones. Fig. 4(a) shows that the self-field $I_c$ of the Fujikura wire is slightly bigger than that of the SHS wire, and $I_c$ of the SHS wire under perpendicular magnetic field degrades slightly faster than that of the Fujikura wire towards high magnetic field. In Fig. 4(b), $I_c$ of

SHS wire and Fujikura wire in parallel magnetic field is similar, even though the SHS wire has a slightly better $I_c$ performance.

Together with (1) and (2), the governing equations are derived from Faraday's law (4), Ampere's law (5), and the constitutive law (6), where $\mu_0$ is vacuum permeability and $\mu_{re}$ is the relative permeability.

$$\nabla \times \boldsymbol{E} = -\partial \boldsymbol{B}/\partial t \tag{4}$$

$$\nabla \times \boldsymbol{H} = \boldsymbol{J} \tag{5}$$

$$\boldsymbol{B} = \mu_0 \mu_{re} \boldsymbol{H} \tag{6}$$

The governing equation (7), written in the form of a partial differential equation (PDE), is computed by COMSOL to solve the magnetic field and current density distributions.

$$\partial(\mu_0 \mu_{re} \boldsymbol{H})/\partial t + \nabla \times \rho(\nabla \times \boldsymbol{H}) = 0 \tag{7}$$

Adding the magnetic field components $H_r$ and $H_z$ into equation (7), we get another type of governing equation to be solved by the COMSOL software, as shown in (8),

$$\begin{cases} \mu_0 \mu_{re} \dfrac{\partial H_r}{\partial t} - \dfrac{1}{r} \dfrac{\partial \left( r\rho \left( \dfrac{\partial H_r}{\partial z} - \dfrac{\partial H_z}{\partial r} \right) \right)}{\partial z} = 0 \\ \mu_0 \mu_{re} \dfrac{\partial H_z}{\partial t} + \dfrac{1}{r} \dfrac{\partial \left( r\rho \left( \dfrac{\partial H_r}{\partial z} - \dfrac{\partial H_z}{\partial r} \right) \right)}{\partial r} = 0 \end{cases} \tag{8}$$

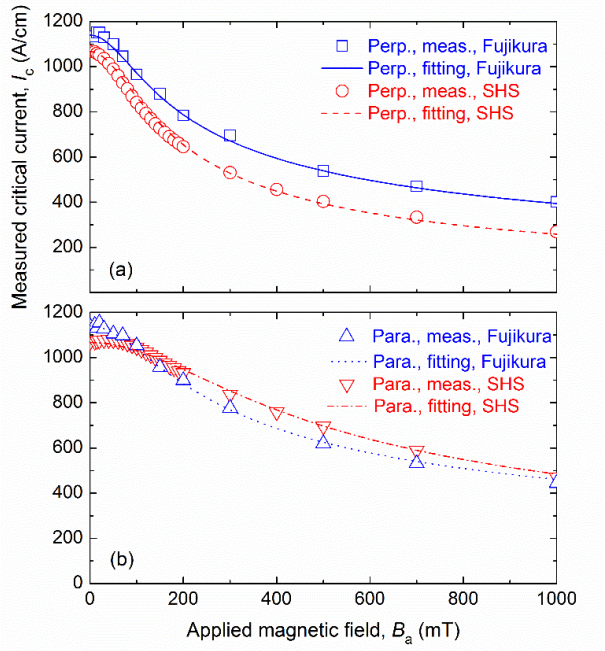


Fig. 4. $I_c$ ($B$) dependence of both Fujikura and SHS wires exposed to external magnetic fields (a) Perpendicular magnetic field (b) Parallel magnetic field.

## III. AC Loss and Discussion

Fig. 5 shows the calculated AC loss result in Conf. #1 wound using Fujikura wire only plotted as a function of $I_{t,\,peak}$ which is the transport current in the LV windings. AC loss values increase approximately with the 3rd power of $I_{t,\,peak}$. At $I_{t,\,peak}$ = $I_{rated}$ = 1234 A, AC loss in the whole transformer winding reaches 3.787 kW.

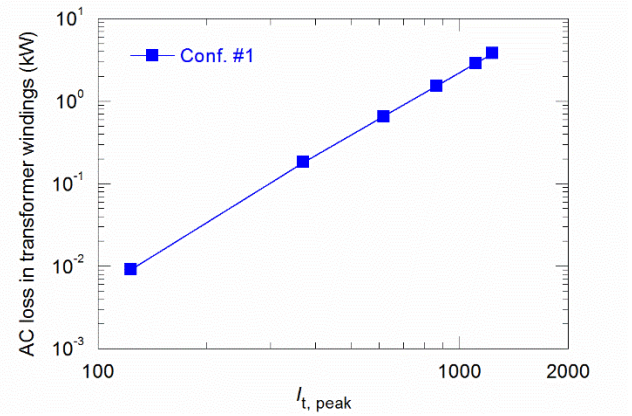


Fig. 5. AC loss results in Conf. #1

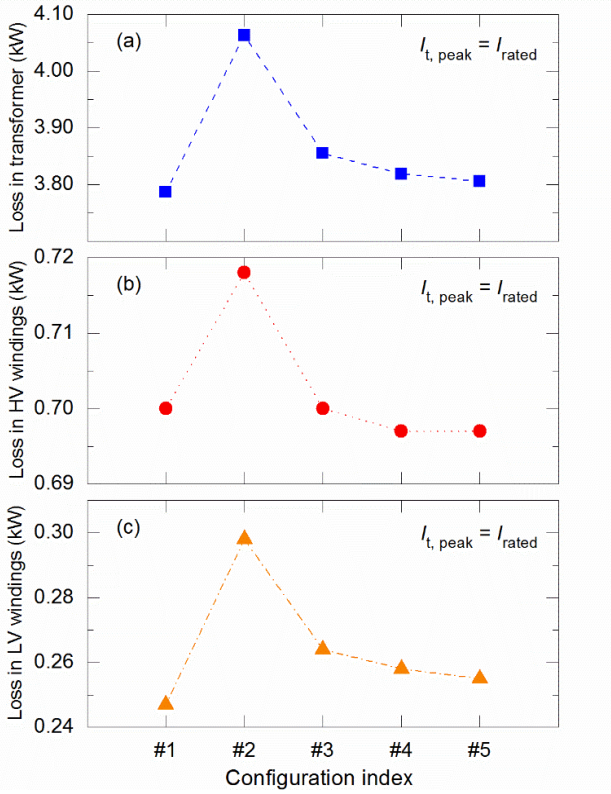


Fig. 6 AC loss comparison in transformer windings, HV winding and LV winding in Confs. #1 through to #5 simulated at the rated current (a) transformer windings, (b) HV winding, and (c) LV winding

In Figs. 6(a), 6(b) and 6(c), the AC loss values in the whole transformer windings, and in HV and LV windings for confs. #1 to #5 at the rated current are compared. Table II also lists the detailed AC loss data shown in Fig. 6. As shown in Fig. 6(a), AC loss in the whole transformer for Conf. #1 is the lowest, peaks for Conf. #2, and drops sharply for hybrid configurations Confs. #3, #4, and #5, with the values decreasing slowly with increasing usage of the Fujikura wire in the end part of the windings. The same tendency holds true for the AC loss in the HV and LV windings as shown in Figs. 6(b) and 6(c). The difference in AC loss values between Conf. #1, which uses all Fujikura wire and Conf. #2 which uses all SHS wire is 7.03% due to the difference in $I_c(B)$ performances in the Fujikura and SHS wires. However, the difference in AC loss values between Conf. #1 and Conf. #3 is only 1.78%, even though Conf. #3 uses only a small portion of the Fujikura wire in the end of the windings.

TABLE II
AC LOSS IN TRANSFORMERS WITH VARIOUS CONFIGURATIONS

| Configu-ration | Loss in transformer windings (kW) | Loss in HV (kW) | Loss in LV (kW) |
|---|---|---|---|
| #1 | 3.787 | 0.700 | 0.247 |
| #2 | 4.063 | 0.718 | 0.298 |
| #3 | 3.855 | 0.700 | 0.264 |
| #4 | 3.819 | 0.697 | 0.258 |
| #5 | 3.806 | 0.697 | 0.255 |

This implies that substantial cost reduction can be achieved with a hybrid winding structure if there is a significant price premium for high- $I_c$ wire; using low cost, relatively low-$I_c$ wire for the majority of the winding while incurring a negligible AC loss increase. The cost benefit will become larger for hybrid windings if there is larger difference in wire price. There are slight differences in AC loss values between the hybrid transformer windings, Confs. #3, #4, and #5, e.g. the difference in AC loss values between Confs. #3 and #5 is only 1.28%, even though Conf. #5 uses twice as much Fujikura wire as Conf. #3. Therefore, Conf. #3 is the best choice, balancing both HTS wire cost and AC loss.

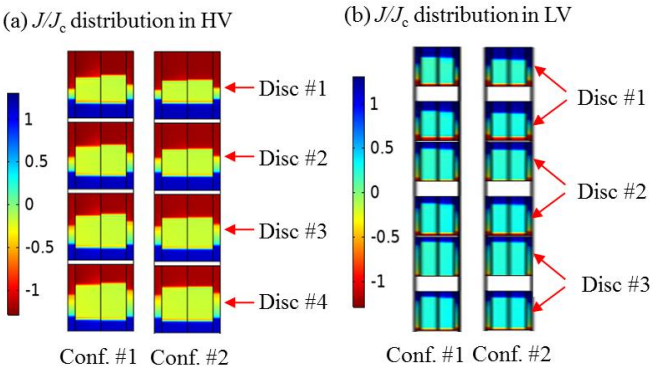


Fig. 7. $J/J_c$ distributions in Confs. #1, #2, #3. (a) HV winding (b) LV winding

Figs. 7(a) and 7(b) show the $J/J_c$ distribution in the top discs of the HV and LV windings of Confs. #1 and #2. In the discs, there is shielding current flowing opposite to coil current in order to shield the radial magnetic field component in the end part of the windings. The region where $|J/J_c| > 1$ has full magnetic field penetration, and the region where $|J/J_c| > 1$ is bigger in Conf. #2 than that in Conf. #1. This explains why the AC loss value in Conf. #2 is larger than that in Conf. #1.

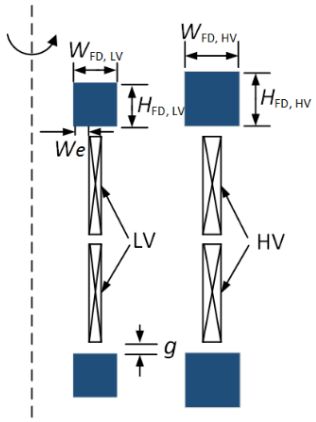


Fig. 8. Schematic of flux diverters at the end part of the HV and LV windings

AC loss in HTS transformers needs to be restrained within 2 kW in order to achieve the efficiency and system weight targets [6]. None of the Confs. #1 to #5 can meet the AC loss requirement, so flux diverters have to be used to shape the magnetic field in the end of the windings in order to reduce the AC loss in the windings [21, 22]. In this work, AC loss in Conf. #6 (Conf. #3 with flux diverters) was calculated.

Fig. 8 shows the schematic of dimensions for flux diverters arranged near the outer ends of the HV and LV windings of Conf. #3. Here, the cross-section of flux diverter was chosen as square and the permeability of magnetic material in the flux diverter has a constant $\mu_{re}$ of 100. $W_e$, $g$, $W_{FD,\,HV}$, and $W_{FD,\,LV}$ are 8.0 mm, 0.5 mm, 20.2 mm, and 17.8 mm, respectively.

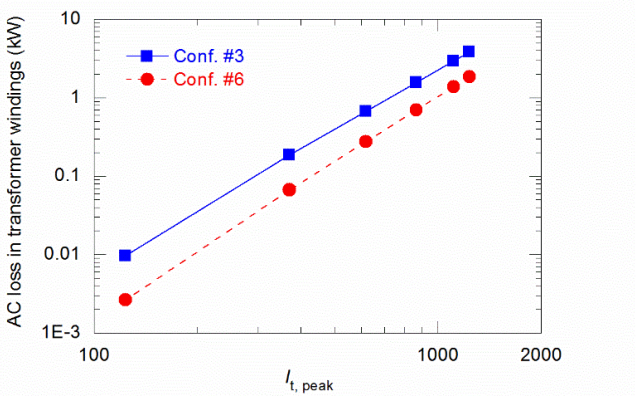


Fig. 9. Comparison of AC loss results in Conf. #3 and Conf. #6.

Fig. 9 compares the calculated AC loss values in Conf. #3 and Conf. #6. AC loss was reduced significantly with flux diverters in place. At rated current, AC loss in Conf. #6 is 1.859 kW, which is less than half of the loss in Conf. #3. This AC loss value meets the AC loss target. It is worth noting that flux diverters have their own eddy current loss and hysteresis loss. More work needs to be done to refine the design of practical and effective flux diverters.

## IV. CONCLUSION

In this paper, a hybrid winding structure has been proposed for a 6.5 MVA/25 kV traction transformer in order to reduce HTS wire cost while achieving acceptably low AC loss.

We calculated and compared six winding configurations, which use different portions of Fujikura wire and SHS wire in the HV and LV windings. By replacing two discs at the outer ends of HV and LV windings with Fujikura wire, while all other central discs are wound using SHS wire, we obtained similar AC loss in the configuration (Conf. #3) as in the configuration wound entirely with Fujikura wire (Conf. #1) .

With flux diverters arranged at the outer ends of the windings of the hybrid configuration Conf. #3, we can get 1.859 kW loss, which is less than our AC loss target for the project.

Since the cost of HTS wire varies by more than a factor of two, depending on manufacturer and wire quality [23], there is potential to halve the total wire cost by using high-cost, high-$I_c$ wire only in the end turns of the windings where the extra performance is needed to constrain the AC loss.

## REFERENCES


[1] M. Leghissa, B. Gromoll, J. Rieger, M. Oomen, H. Neumüller, R. Schlosser, H. Schmidt, W. Knorr, M. Meinert, and U. Henning, "Development and application of superconducting transformers," *Phys. C* vol. 372, pp. 1688-1693, 2002.

[2] R. Schlosser, H. Schmidt, M. Leghissa, and M. Meinert, "Development of high-temperature superconducting transformers for railway applications," *IEEE Trans. Appl. Supercond*., vol. 13, no. 2, pp. 2325-2330, Jun. 2003.

[3] H. Kamijo, H. Hata, H. Fujimoto, K. Ikeda, T. Herai, K. Sakaki, H. Yamada, Y. Sanuki, S. Yoshida, Y. Kamioka, M. Iwakuma, and K. Funaki, "Fabrication of inner secondary winding of high-Tc superconducting traction transformer for railway rolling stock," *IEEE Trans. Appl. Supercond*., vol. 15, no. 2, pp. 1875-1878, Jun. 2005.

[4] H. Hata, H. Kamijo, K. Nagashima, and K. Ikeda, "Development of superconducting transformer for railway traction," *In Electrical Systems for Aircraft, Railway and Ship Propulsion*, pp. 1-4, 2010, Art. no. 5665211.

[5] W. Song, J. Fang, Z. Jiang, M. Staines, and R. Badcock, "AC Loss Effect of High-Order Harmonic Currents in a Single-Phase 6.5 MVA HTS Traction Transformer," *IEEE Trans. Appl. Supercond.*, vol. 29, no. 5, Art. no. 5501405, Aug. 2019.

[6] W. Song, Z. Jiang, M. Staines, S. Wimbush, R. Badcock, J. Fang, J. Zhang, "Design of a Single-Phase 6.5 MVA/25 kV Superconducting Traction Transformer for the Chinese Fuxing High-Speed Train," *Int. J. Electr.. Power Energy Syst.*, under review.

[7] X. Li, J. Zhang, K. Huang, X. Song, and J. Fang, "Electromagnetic design of high-temperature superconducting traction transformer for high-speed railway train," *IEEE Trans. Appl. Supercond*., vol. 29, no. 5, pp. 1-5, 2019.

[8] M. Yazdani-Asrami, M. Staines, G. Sidorov, et al., "Fault current limiting HTS transformer with extended fault withstand time", *Supercond. Sci. Technol*., vol. 32, Art. no. 035006, 2019.

[9] W. Goldacker, F. Grilli, E. Pardo, A. Kario, S. I. Schlachter, and M. Vojenčiak, "Roebel cables from REBCO coated conductors: a one-century-old concept for the superconductivity of the future," *Supercond. Sci. Technol*., vol. 27, no. 9, Art. no. 093001, 2014.

[10] N. J. Long, R. A. Badcock, K. Hamilton, A. Wright, Z. Jiang, and L. S. Lakshmi, L. S, "Development of YBCO Roebel cables for high current transport and low AC loss applications," *J. Phys. Conf. Ser*., vol. 234, no. 2, Art. no. 022021, 2010.

[11] N. Glasson, M. Staines, Z. Jiang, and N. Allpress, "Verification testing for a 1 MVA 3-phase demonstration transformer using 2G-HTS Roebel cable," *IEEE Trans. Appl. Supercond*., vol. 23, no. 3, Art. no. 5500206, Jun. 2013.

[12] E. Pardo, M. Staines, Z. Jiang, and N. Glasson, "Ac loss modelling and measurement of superconducting transformers with coated-conductor Roebel-cable in low-voltage winding," *Supercond. Sci. Technol*., vol. 28, no. 11, Art. no. 114008, Oct. 2015.

[13] W. Song, Z. Jiang, X. Zhang, M. Staines, R. Badcock, J. Fang, Y. Sogabe, N. Amemiya, "AC loss simulation in a HTS 3-Phase 1 MVA transformer using H formulation," *Cryogenics*, vol. 94, pp. 14-21, 2018.

[14] Z. Jiang, N. Long, M. Staines, R. A. Badcock, C. W. Bumby, R. G. Buckley, and N. Amemiya, "AC loss measurements in HTS coil assemblies with hybrid coil structures," *Supercond. Sci. and Technol.*, vol. 29, Art. no. 095011, 2016.

[15] Z. Jiang, M. Staines, N. J. Long, R. A. Badcock, C. W. Bumby, R. G. Buckley, W. Song, and N. Amemiya, "AC loss measurements in a hybrid REBCO/BSCCO coil assembly," *IEEE Trans. Appl. Supercond*., vol. 27, no. 6, Art. no. 5900707, Sep. 2017.

[16] Z. Hong, A. M. Campbell, and T. A. Coombs, "Numerical solution of critical state in superconductivity by finite element software," *Supercond. Sci. and Technol.*, vol. 19, pp. 1246–1252, 2006.

[17] R. Brambilla, F. Grilli, and L. Martini, "Development of an edge-element model for AC loss computation of high-temperature superconductors," *Supercond. Sci. and Technol.*, vol. 20, pp. 16–24, Nov. 2006.

[18] V. M. R. Zermeno, N. Mijatovic, C. Træholt, T. Zirngibl, E. Seiler, A. B. Abrahamsen, N. F. Pedersen, and M. P. Sorensen, "Towards faster FEM simulation of thin film superconductors: a multiscale approach," *IEEE Trans. Appl. Supercond*., vol. 21, pp. 3273–3276, 2011.

[19] M. Zhang, J. H. Kim, S. Pamidi, M. Chudy, W. Yuan, and T. A. Coombs, "Study of second generation, high-temperature superconducting coils: Determination of critical current," *J. Appl. Phys.*, vol. 111, no. 8, Art. no. 083902, 2012.

[20] Y. B. Kim, C. F. Hempstead, and A. R. Strnad, "Critical persistent currents in hard superconductors," *Phys. Rev. Lett.*, vol. 9, pp. 306–309, 1962.

[21] J. K. Sykulski, K. F. Goddard, and R. L. Stoll, "A method of estimating the total AC loss in a high-temperature superconducting transformer winding," *IEEE Trans. Magn*., vol. 36, no. 4, pp. 1183-1187, 2000.

[22] E. Pardo, J. Šouc, and M. Vojenčiak, "AC loss measurement and simulation of a coated conductor pancake coil with ferromagnetic parts," *Supercond. Sci. Technol*., vol. 22, no. 7, Art. No. 075007, 2009.

[23] S. C. Wimbush, N. M. Strickland, M. P. Staines, Z. Jiang, R. C. Mataira, N. J. Long and R. A. Badcock, "Informed wire selection for an HTS traction transformer," Presentation 3LPo1G-01, Applied Superconductivity Conference, Seattle USA, 28 October – 2 November 2018.